

Real-time, T-Ray Imaging Using a Sub-Terahertz Gyrotron

Seong-Tae HAN*

Korea Electrotechnology Research Institute, Ansan 426-170, Korea

Antonio C. TORREZAN, Jagadishwar R. SIRIGIRI, Michael A. SHAPIRO and Richard J. TEMKIN
Massachusetts Institute of Technology, Cambridge, MA 02139, USA

(Received 26 March 2012, in final form 24 April 2012)

We demonstrated real-time, active, T-ray imaging using a 0.46 THz gyrotron capable of producing 16 W in continuous wave operation and a pyroelectric array camera with 124-by-124 pixels. An expanded Gaussian beam from the gyrotron was used to maintain the power density above the detection level of the pyroelectric array over the area of the irradiated object. Real-time imaging at a video rate of 48 Hz was achieved through the use of the built-in chopper of the camera. Potential applications include fast scanning for security purposes and for quality control of dry or frozen foods.

PACS numbers: 07.57.Hm, 84.47.+w, 87.63.-d, 89.20.-a

Keywords: T-ray, Real-time imaging, Sub-terahertz, Gyrotron

DOI: 10.3938/jkps.60.1857

I. INTRODUCTION

T-ray (terahertz wave) imaging has received constantly growing interest as a promising method in security screening, quality control of food products and numerous other applications [1,2]. Nevertheless, the lack of a powerful source and a more sensitive detector has been an obstacle to realizing such a potential imaging modality in the real world. To overcome the limited availability of powerful source, conventional terahertz (THz) active imaging systems employ a focused point-beam scanned over the object regardless of the kind of source [3–6], which results in a long scanning time to take a frame of the image. Because a long image-acquisition time cannot satisfy the demands for practical applications, a real-time two-dimensional imaging method has been investigated by many researchers.

An electro-optic (EO) sampling technique converting the pulsed THz field from a photoconductive antenna to an optical intensity by using an EO crystal for recording by a CCD camera was applied to reduce the acquisition time, and high-speed THz imaging was successfully demonstrated in real time [7]. In real-world applications, however, this approach might suffer from the lack of stand-off-detection capability.

On the other hand, active real-time T-ray imaging has been demonstrated by using a micro-bolometer focal plane array camera with single-frequency continuous-wave (CW) sources, such as far-infrared gas lasers

(2.52 THz) [8] or quantum cascade lasers (QCLs) (4.3 THz) [9]. In spite of the successful demonstration of stand-off detection, the gas laser and the QCL should be enhanced toward the lower frequency region of the THz spectrum because the sub-THz region is preferred for inspection purposes in that materials common in garments and packing become progressively opaque in the higher frequency THz region [10]. In addition, the performance of the gas laser and the QCL need further improvement even in the higher THz region to compete successfully against the extremely low sensitivity of the micro-bolometer array camera optimized for wavelengths of 7.5 – 14 μm [11].

For better spatial resolution of the T-ray image, a higher frequency is preferred even though transmission through clothing and packing decreases as the frequency increases. A subterahertz signal should be more suited as a trade-off between penetration and resolution. However, the sensitivity of array detectors operating in this frequency region is relatively low; for example, the sensitivity of the pyroelectric camera is about 300-mW/cm² at around 1 THz at room temperature [12]. Besides, most existing, relatively-low-power sub-THz sources only provide weak beams, which make detection slower and harder. Therefore, the ideal system for practical applications requires radiation sources at lower THz frequencies with superior output power to illuminate the entire inspection area with a wide field-of-view while maintaining the power density above the detection level of a focal plane array camera operating with low sensitivity at room temperature.

*E-mail: saiph@keri.re.kr; Fax: +82-31-8040-4189

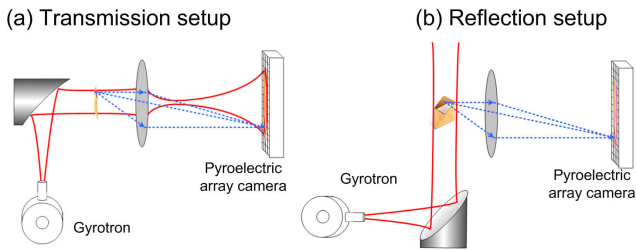


Fig. 1. (Color online) Layouts for the active terahertz real-time imaging system: The terahertz beam (solid profile) is expanded and collimated by the off-axis parabolic mirror and irradiates the objects under test. The scattered energy (dotted line) from each part of the object is imaged by the pyroelectric detector array.

Generally, the approach to achieving source power around the above frequency range has been either to use multipliers to generate radiation from RF sources [5] or to translate down in frequency from the optical region by using a laser and nonlinear medium, such as optically-pumped gas lasers [8], photomixing [3], and parametric oscillators [13]. Alternatively, backward wave oscillators [4] and quantum cascade lasers [9] have been taken into consideration. If the practical requirement for a T-ray imaging system operating in the sub-THz region is to be satisfied, however, listed sources need further enhancement in attaining high-power capability. As a possible solution, an active, real-time, imaging system employing a CW sub-THz gyrotron [14], in conjunction with a commercially available pyroelectric array camera [12], is proposed in this paper.

This paper is organized as follows: In Sec. II, the details of the experimental configuration for the T-ray imaging are described. The capability of real-time T-ray imaging is demonstrated in Sec. III, where captured and processed images from videos of a moving paper envelope containing metallic letters inside are presented. Finally, discussions on the availability of the proposed T-ray-imaging system are provided.

II. EXPERIMENTAL CONFIGURATION

A quasi-optical schematic of the proposed system for active, real-time T-ray imaging is depicted in Fig. 1. The TEM_{00} -like output beam from the sub-THz gyrotron is expanded by using an off-axis parabolic mirror after a corrugated waveguide, and the collimated beam illuminates a passing object under test at a distance. The transmitted or the reflected beam is captured by a teflon lens in the active area of detector arrays instead of imaging one pixel at a time.

The image size is constrained by the size of the detector arrays. This experiment employs a pyroelectric camera [7] consisting of an array of 124-by-124 $LiTaO_3$

pyroelectric sensors (originally designed for laser applications) with a spacing of $100 \mu m$ between each pixel and a motorized chopper over the sensor array [12]. The pyroelectric camera is a reliable and commercially-available array detector, though its sensitivity in the terahertz range is poor, and it is too small to provide images of large targets. The built-in chopper enables the pyroelectric crystals to detect CW beams by using the changes in the signal against the background. The pyroelectric crystal only measures changes in intensity, so it is relatively immune to ambient temperature changes, unlike a microbolometer array, which requires a constant temperature bath. Pyroelectric detectors are ideally suited, because they generate a signal proportional to the rate of change of temperature and give no signal when in thermal equilibrium. For this experiment, a chopping frequency of 48 Hz was selected. The sensitivity in the sub-THz region is enhanced by introducing a filter of thin polyethylene in front of the detector to prevent background infrared radiation from overwhelming the sub-THz signals.

The gyrotron, in other words, electron cyclotron resonance maser (ECRM), is a coherent radiation source using the resonance between the cyclotron motion (gyration) of the electrons in a strong magnetic field and the Doppler-shifted frequency of the electromagnetic field in a resonant cavity. This resonance gives rise to the so-called electron cyclotron maser instability, which depends on the electron cyclotron frequency. Provided that the Doppler-shifted radiation frequency is slightly higher than the cyclotron frequency or its harmonics, the electrons experience azimuthal phase bunching, and the formed bunches slip naturally into a decelerating phase where they transfer some of their transverse energy to the wave through a Bremsstrahlung interaction [15].

Although optically-pumped lasers offer useful power levels in the sub-THz band, they are limited for many applications because they operate only on discrete frequencies and because the pulsed versions have a low duty cycle. Contrarily, the gyrotron is capable of frequency selection at the designers' will, accounting for the effect of atmospheric window and minimal attenuation by the materials under inspection. A CW system tuned to a spectral window between atmospheric absorption lines is easier to operate at longer standoff distances. The inherent stability of the gyrotron with a narrow line-width is another figure of merit [16] to be mentioned. Therefore, it is most effective when a gyrotron is used as the irradiation source in conjunction with an insensitive sensor to take real-time images at the video rate due to its inherent high power capability in that frequency range with good output beam pattern for covering a wide inspection space.

Figure 2 shows an image of the TEM_{00} -like mode pattern captured at 40 mm after the end of the corrugated waveguide from a 0.46-THz CW gyrotron capable of producing 16 Watts in CW operation with a 13-kV 100-mA electron beam [14]. The gyrotron is operated at the second cyclotron-harmonic, which eases the magnetic field

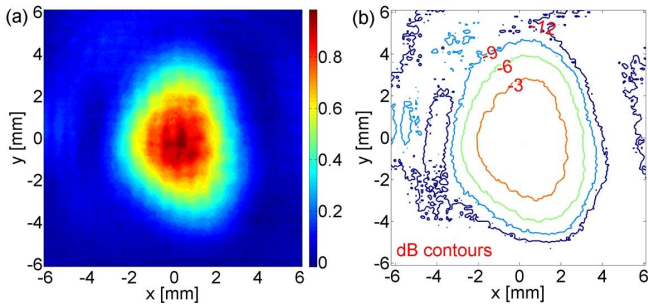


Fig. 2. (Color online) Gyrotron output beam displayed on a (a) normalized linear power scale and a (b) dB contours. The pyroelectric camera image of the mode-converted $TE_{11,2}$ mode at 0.46 THz was taken 40 mm after the end of the corrugated waveguide. The power was limited to 0.4 W below the damage threshold of the sensing element.

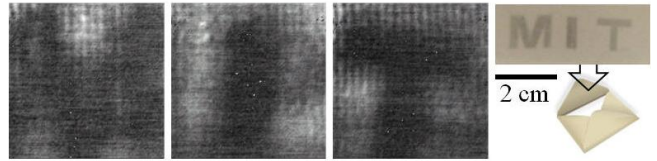
requirement and results in a relatively compact system. Based on the measured pattern, the Gaussian-like content associated with the measured terahertz beam was computed to be 92%, with beam radii $w_x = 4.1$ mm and $w_y = 4.6$ mm, corresponding to an ellipticity of 12%. Measurements performed with thermal paper corroborated the camera results. These results indicate a good spatial performance of the output beam generated by the gyrotron through the use of an internal quasi-optical mode converter converting a whispering-gallery mode of the gyrotron cavity ($TE_{11,2}$ mode) to a Gaussian-like beam.

III. T-RAY IMAGING IN REAL-TIME

As a demonstration of the capability of a real-time T-ray imaging system to see through visually opaque material, we take real-time videos of a moving, paper mailing envelope containing metallic letters with the transmission and the reflection setups, respectively. The beam shown in Fig. 1 is expanded to illuminate the sample homogeneously with the power density below the saturation level of the pyroelectric array detector (3.2 W/cm^2). The intensity captured in the camera without any sample is about 10 dB below the peak intensity under the condition of 32 (2^5) times multiplication. Therefore, reasonably the sample is thought to be illuminated with a power density of more than 10 mW/cm^2 when the loss along the optical path, including the lens, is considered.

Because the principle of the array camera is to detect alternating signals in the pyroelectric elements by using a built-in chopper over the detection plane, each frame can be obtained in accordance with the frequency of the chopper. For this measurement, a video is recorded at a rate of 48 fps (frames per second). To prove the capability of real-time imaging, we use a maximum 48 fps in taking the video, though clearer images can be obtained at lower frame rate by averaging several frames. Mov-

(a) Captured images (“MIT” by transmission)



(b) Captured images (“KERI” by reflection)

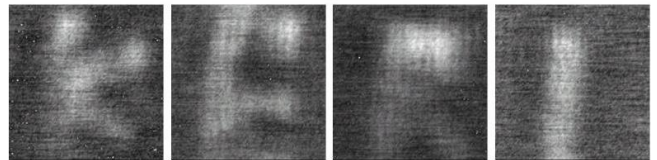


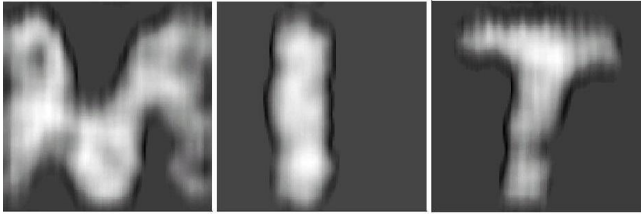
Fig. 3. Images captured from real-time videos taken in the setup of (a) transmission (“MIT” acronym for Massachusetts Institute of Technology) and (b) reflection (“KERI” acronym for Korea Electrotechnology Research Institute). Letters identified by the terahertz imaging system are contained in the visually opaque paper mailing envelop. (The example photograph of the metallic letters formed with aluminum foil and the configuration are demonstrated at the top-right corner.) The thickness of each stroke of the letters is about 2 – 3 mm to avoid diffraction. Experiment using a series of slits with different thickness indicated that at least more than 1 mm is necessary to identify the pattern in the image obtained with the present system.

ing the sample in Fig. 3(a), one can clearly identify the objects inside the envelope in the real-time videos with a running time of just a few seconds. Employed with a larger detector, objects can be identified even in a single shot. Figure 3 shows individual frames taken from the videos showing detected images of letters made of metallic foil and hidden inside a paper envelope. These results show that it is possible to detect metallic objects hidden in clothing or similar materials.

The etalon effect (bright and dark interference fringes), which is inherent in the images taken with a coherent, monochromatic radiation source, is clearly visible in Fig. 3(b). It may be attributed to multiple reflections of the high-power-density beam between the detector and the lens in the parallel configuration for the transmission measurement. Reflective optical elements, instead of the lens, might reduce spurious reflections, and consequently, reduce the etalon effect

Due to the low sensitivity of the array detectors, the captured images have low signal-to-noise ratios. Thus, the contrast along the edges of the images is enhanced by rounding off the intensity fluctuations consisting of noise (see Fig. 4(a)). Figure 4 shows a comparison between the images of “MIT” obtained by (a) transmission (different frame from Fig. 3) and (b) reflection. The black and the white of the image obtained by transmission is inverted to be directly compared with the image obtained by reflection. The result clearly shows that in the transmission configuration, background sub-terahertz energy entering

(a) Inverted and contrast enhanced transmission image



(b) Contrast enhanced reflection image

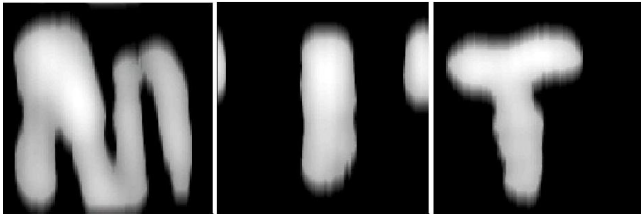


Fig. 4. Comparison between the images of “MIT” obtained by (a) transmission and (b) reflection: The contrast along the edge of the images is enhanced by rounding off the intensity fluctuations consisting of noise. The black image by (a) transmission is inverted to a white image to be directly compared with the one by (b) reflection.

the detector raises the overall noise floor. The reflection configuration provides better contrast thanks to the absence of background irradiation and suffers less from the etalon effect, though the width is contracted because of tilting in the configuration.

IV. CONCLUSION AND OUTLOOK

We demonstrated real-time, active, T-ray imaging using a sub-THz gyrotron capable of producing high power to overcome the limit of the sensitivity of the array detectors available for this frequency region. In recent years, gyrotron technology has been moving towards compact systems that have smaller footprints and can be rapidly deployed. The development of sub-THz wave gyrotrons for applications in electron paramagnetic resonance (EPR) and dynamic nuclear polarization (DNP) [16] has resulted in gyrotrons operating at the second to third cyclotron harmonic, which reduces the magnetic field requirement due to the harmonic number. These devices operate at low voltages in the 10-kV range with a prime power requirement of about 1 kW. This modern gyrotron technology is very compact, and its high CW output power capability in the 0.2-THz to 1-THz range is uniquely suited for a number of homeland security applications where stand-off distance is a prime requirement. The continuous evolution of superconducting magnet technology, especially in liquid-cryogen-free systems, will allow further reduction in the size and the cost of gyrotron systems for imaging applications. With current gyrotron technology, it is possible to produce

10-W CW power at 0.5 THz by using a system of less than 1 cubic meter in volume. If real-time operation of imaging is to be achieved with the limited sensitivity of commercially-available array detectors, the sub-terahertz gyrotron is a promising source capable of illuminating an area of the focal plane area of several to many square centimeters while maintaining the power density above the detection level.

The proposed active, real-time, T-ray imaging method should be especially suited for applications such as fast security screening and quality control of food. Even in these early-stage laboratory experiments, we were able to see that it might be possible to meet the compelling needs for real-time stand-off detection of concealed weapons on people at security-check points, and for identification of a foreign substance in visually opaque dry or frozen food on a production line. Ultimately, it is hoped that this proposed technology will gain more widespread acceptance in future systems.

ACKNOWLEDGMENTS

This work was supported partly by the Joint Research Project of ISTK (Korea Research Council for Industrial Science and Technology). Also, this work was supported in part by the National Institute of Health (NIH) and National Institute of Biomedical Imaging and Bioengineering (NIBIB) under contract EB004866.

REFERENCES

- [1] National Research Council (U.S.), Assessment of Millimeter-Wave and Terahertz Technology for Detection and Identification of Concealed Explosive and Weapons (The National Academies Press, 2007).
- [2] M. Tonouchi, *Nat. Photonics* **1**, 97 (2007).
- [3] K. J. Siebert, H. Quast, R. Leonhardt, T. Löffler, M. Thomson, T. Bauer and H. G. Roskos, *Appl. Phys. Lett.* **80**, 3003 (2002).
- [4] A. Dobroiu, M. Yamashita, Y. N. Ohshima, Y. Morita, C. Otani and K. Kawase, *Appl. Opt.* **43**, 15637 (2004).
- [5] N. Karpowicz, H. Zhong, C. L. Zhang, K-I Lin, J-S. Hwang, J. Xu and X-C. Zhang, *Appl. Phys. Lett.* **86**, 054105 (2005).
- [6] K. Shibuya, M. Tani, M. Hangyo, O. Morikawa and H. Kan, *Appl. Phys. Lett.* **90**, 161127 (2007).
- [7] Q. Wu, T. D. Hewitt and X-C. Zhang, *Appl. Phys. Lett.* **69**, 1026 (1996).
- [8] A. W. M. Lee and Q. Hu, *Opt. Lett.* **30**, 2563 (2005).
- [9] A. W. M. Lee, B. S. Williams, S. Kumar and Q. Hu, *IEEE Photon. Technol. Lett.* **18**, 1415 (2006).
- [10] J. E. Bjarnason, T. L. J. Chan, A. W. M. Lee, M. A. Celis and E. R. Brown, *Appl. Phys. Lett.* **85**, 519 (2004).
- [11] N. Butler, R. Blackwell, R. Murphy, R. Silva and C. Marshal, *Proc. SPIE* **2552**, 583 (1995).

- [12] Pyrocam III, Model PY-III-C-B (Spiricon, Inc.).
<http://www.ophir-spiricon.com/laser-measurement-instruments/beam-profilers/products/industrial-applications/cameras/pyroelectric-array-cameras/1>.
- [13] K. Kawase, *Opt. Photonics News* **15**, 3 (2004).
- [14] A. C. Torrezan, S. T. Han, M. A. Shapiro, J. R. Sirigiri and R. J. Temkin, in *Proceedings of International Conference on Infrared, Millimeter, and THz waves* (Pasadena, California, 2008), p. 15.
- [15] G. S. Nusinovich, *Introduction to the Physics of Gyrotrons* (Johns Hopkins, Baltimore, 2004).
- [16] S. T. Han, C. D. Joye, I. M. Mastovsky, M. A. Shapiro, J. R. Sirigiri, R. J. Temkin, A. C. Torrezan and P. P. Woskov, *Proc. SPIE* **6373**, 63730C-1 (2006).